

AFRL-VS-TR-2000-1545
E.R.P., No. 1236

**MASTER DATA BASE FOR OPTICAL TURBULENCE
RESEARCH IN SUPPORT OF AIRBORNE LASER**

Allan J. Bussey
John R. Roadcap, Lt. Col., USAF
Robert R. Beland
George Y. Jumper, Jr.

April 2000

APPROVED FOR PUBLIC RELEASE; DISTRIBUTION UNLIMITED.

20010417 049

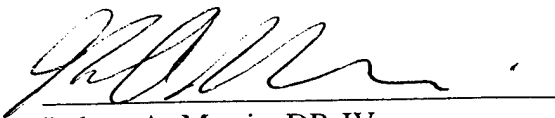


AIR FORCE RESEARCH LABORATORY
Space Vehicles Directorate
29 Randolph Rd.
AIR FORCE MATERIEL COMMAND
HANSCOM AIR FORCE BASE, MA 01731-3010

"This technical report has been reviewed and is approved for publication."



ROBERT R. BELAND
Chief, Tactical Environmental Support Branch
Battlespace Environment Division



Robert A. Morris, DR-IV
Acting Chief, Battlespace Environment Division
Space Vehicles Directorate

This document has been reviewed by the ESC Public Affairs Office (PA) and is releasable to the National Information Service (NTIS).

Qualified requesters may obtain additional copies from the Defense Technical Information Center (DTIC). All others should apply to the NTIS.

If your address has changed, if you wish to be removed from the mailing list, or if the addressee is no longer employed by your organization, please notify AFRL/VSR, 29 Randolph Road, Hanscom AFB, MA 01731-3010. This will assist us in maintaining a current mailing list.

Do not return copies of this report unless contractual obligations or notices on a specific document requires that it be returned.

REPORT DOCUMENTATION PAGE

*Form Approved
OMB No. 0704-0188*

Public reporting burden for this collection of information is estimated to average 1 hour per response, including the time for reviewing instructions, searching existing data sources, gathering and maintaining the data needed, and completing and reviewing the collection of information. Send comments regarding this burden estimate or any other aspect of this collection of information, including suggestions for reducing this burden, to Washington Headquarters Services, Directorate for Information Operations and Reports, 1215 Jefferson Davis Highway, Suite 1204, Arlington, VA 22202-4302, and to the Office of Management and Budget, Paperwork Reduction Project (0704-0188), Washington, DC 20503.

1. AGENCY USE ONLY (Leave blank)		2. REPORT DATE 1 May 2000	3. REPORT TYPE AND DATES COVERED Scientific Interim, Oct 99-Apr 00	
4. TITLE AND SUBTITLE Master Data Base for Optical Turbulence Research in Support of Airborne Laser			5. FUNDING NUMBERS PE: 63319F PR: ABL0 TA: TS WU: 88	
6. AUTHOR(S) Allan J. Bussey, John R. Roadcap, Robert R. Beland, George Y. Jumper, Jr.				
7. PERFORMING ORGANIZATION NAME(S) AND ADDRESS(ES) Air Force Research Laboratory/VSBLL 29 Randolph Rd. Hanscom AFB, MA 01731-3010			8. PERFORMING ORGANIZATION REPORT NUMBER AFRL-VS-TR-2000-1545 E.R.P., No. 1236	
9. SPONSORING/MONITORING AGENCY NAME(S) AND ADDRESS(ES)			10. SPONSORING/MONITORING AGENCY REPORT NUMBER	
11. SUPPLEMENTARY NOTES				
12a. DISTRIBUTION AVAILABILITY STATEMENT Approved for Public Release; Distribution Unlimited			12b. DISTRIBUTION CODE	
13. ABSTRACT (Maximum 200 words) A Master Data Base was assembled in support of the Airborne Laser Program (ABL). The database consists of two major tables of data, several forms to facilitate data entry and viewing, some queries of the database, and some reports based on the database. The data which comprises the tables was taken either directly from the world-wide data retrieval campaign taken in support of the ABL or from various meteorological data sources used to better understand the atmospheric conditions that prevailed during the campaign. A description of the Data Tables and how these data were compiled is the thrust of this report.				
14. SUBJECT TERMS optical turbulence thermosonde weather parameters			15. NUMBER OF PAGES 33	
			16. PRICE CODE	
17. SECURITY CLASSIFICATION OF REPORT UNCLASSIFIED	18. SECURITY CLASSIFICATION OF THIS PAGE UNCLASSIFIED	19. SECURITY CLASSIFICATION OF ABSTRACT UNCLASSIFIED	20. LIMITATION OF ABSTRACT SAR	

Contents

1. INTRODUCTION.....	1
2. MASTER FLIGHTS TABLE	1
2.1 Flight, Date, and Time	1
2.2 ZF, Winds, Bottom C_n^2 , Top C_n^2	2
2.3 Trop(1), Trop(2), Trop(3).....	3
2.4 Max (m/s)	3
2.5 200V(m/s), 200Vg(m/s), 200Vag(m/s), 200Vag/V(m/s), Vag Strength.....	3
2.6 Shear Peaks.....	10
2.7 Jet Speed (m/s), Jet Altitude (km).....	10
2.8 North, South, East, West, In Jet, Jet Type, Jet (m/s)	13
2.9 Weather, Surface Temperature (C), Frontal Passage, Sea-Level Pressure (mb), Wind(m/s), Relative Humidity (%).....	16
2.10 Jet Enhancement, Tropospheric Enhancement, Stratospheric Enhancement	16
2.11 Deformation, Intensity.....	18
2.12 Mountain Wave Intensity	21
2.13 Aircraft, RFI, Comments.....	23
3. OPTICAL TURBULENCE DATA REDUCTION AND STORAGE	23
3.1 Data Source.....	23
3.2 Data Preparation for Table	24
4. CAMPAIGN SUMMARY TABLE	26
5. CONCLUSION.....	27

Illustrations

1. Temperature (C) vs. Z (Height (km)) Solid Line and Relative Humidity (%) vs. Z (Height (km)) Dashed Line for HMNSP107.....	4
2. The 200 mb. Geopotential Height Chart Used to Determine the Radius of Curvature for ROKSU022	7
3. The 200 mb. Geopotential Height Chart Used to Determine the Radius of Curvature for ROKSU027	9
4. Vertical Shear (s^{-1}) vs. Altitude (km) at 7, 9, 11 and 13 Point Smoothing for ROKFA115.....	11
5. Vertical Shear (s^{-1}) vs. Altitude (km) at 11 Point Smoothing for ROKFA115.....	12
6. Path of Balloon Sounding from Surface to 38 Km for ROKFA115.....	14
7. 200 mb. Winds (m/s) for ROKFA115 Showing Site Launch and Position of Balloon at 200 mb. Level.....	15
8. C_n^2 (20 Gaussian Average) vs. Z (Height (km)) for HMNSP104. CLEAR 1 Model Superimposed For Comparison.....	17
9. 200 mb. U – Wind Component (m/s) for ROKSP101 with 2° Latitude Radius Circle Drawn over Osan AB, Korea.....	19
10. 200 mb. V – Wind Component (m/s) for ROKSP101 with 2° Latitude Radius Circle Drawn over Osan AB, Korea.....	20
11. Mountain – Wave Nomogram Used to Determine Mountain – Wave Intensity.....	22

Tables

1. Table of Flight Bins and Computed Means.....	26
---	----

Acknowledgment

We thank Kris Robinson and George Clement for the contractual support they provided without which the field campaigns would not have been possible. We also recognize Paul Tracy, Sandra Lewis, Seymour Tompkins, Edmund Murphy and Michael Currie who provided invaluable in-house support both on-site and in the field for the data collection effort. Finally, we thank our colleagues in the Tactical Environment Support Branch for comments and suggestions.

MASTER DATA BASE FOR OPTICAL TURBULENCE RESEARCH IN SUPPORT OF AIRBORNE LASER

1. INTRODUCTION

The C_n^2 Master Database was assembled in support of the Airborne Laser System Program Office (ABL SPO). The database consists of two major tables of data, several forms to facilitate data entry and viewing, some queries of the database, and some reports based on the database. The database is in Microsoft Access format. This report describes the two major tables in the database: The Master Flights Table and the Altitude Bins Table. The Master Flights Table contains the date, time, and location of each balloon launch and various parameters, mostly weather-related, recorded for each flight, either determined in the field or computed later. The Altitude Bins Table is a consolidation of the Thermosonde optical turbulence data from each flight. A third table entitled Campaign is a handy summary of each campaign and the status of the data reduction for that campaign. This report describes these three tables in detail, including the computational methods used in preparing the table entries.

2. MASTER FLIGHTS TABLE

By selecting the Master Flights Table, and clicking the Open button, the entire table can be viewed. To view the data for a single flight, open the Master Flight Viewer Form.

2.1. Flight, Date, and Time

"A"	"B"	"C"
Flight	Date	Time
BAHSP001	6/1/97	8:18:00 PM

An eight digit identifier was assigned to each balloon launch. The first three characters identify the location where the launch occurred; the next two characters indicate the season during which the launch was made; the sixth digit is used to designate more than one campaign for a particular season, and the last two digits number each launch made during the particular campaign.

For example: BAHSP001 corresponds to Bahrain, Spring, launch number one; ROKWN102 is Korea, Winter, launch number two; RUHFA103 is Saudi Arabia, Fall, launch number three; and HMNSP110 is Holloman, Spring, launch number ten. ROKWN102, RUHFA103 and HMNSP110 all designate the first campaign for that Location. This "flight" data was recorded in column number A. The "date" of each launch was recorded in column B and the "time" of each launch (Local time) was listed in column C.

2.2. ZF, Winds, Bottom C_n^2 , Top C_n^2

"D"	"E"	"F"	"G"
ZF	Wind	Bottom C_n^2	Top C_n^2
30	y	0	30

Column D contains "ZF" which is the maximum height (in kilometers) that the balloon attained in the launch during which data were collected for C_n^2 . A value of 0 km indicates that the balloon was not launched successfully.

If wind data were taken it is shown as a "y" value in column E; if no wind data were taken for the launch it is shown as an "n" value in column E.

Bottom C_n^2 , in column F, is the beginning height (km) for which C_n^2 values were taken for the launch. The greatest height (km) for which C_n^2 values were taken is recorded in column G.

2.3. Trop(1), Trop(2), Trop(3)

"H"	"I"	"J"
Trop(1)	Trop(2)	Trop(3)
17.5	0	0

Columns H, I, and J give the height (km) of the tropopause; either single, double, or triple. The tropopause was determined by examining the temperature profile of the sounding. Figure 1 shows a double tropopause for the Spring 98 campaign at Holloman AB, New Mexico. As depicted by the temperature curve (solid line) there is an abrupt change in the decrease in temperature at 13 km and again at 19 km. This dramatic change in the rate of temperature decrease gives merit to a Trop(1) at 13 km and a Trop(2) at 19 km.

2.4. Max (m/s)

"K"
Max(m/s)
33

The maximum wind speed (m/s) recorded by the wind data taken for the flight is given in column K.

2.5. 200V(m/s), 200V_g (m/s), 200V_{ag} (m/s), 200V_{ag}/V(m/s), V_{ag} Strength

"L"	"M"	"N"	"O"	"P"
200V(m/s)	200V _g (m/s)	200V _{ag} (m/s)	200V _{ag} /V(m/s)	V _{ag} strength
35	29.2	-5.8	-0.17	W

The next five columns (L-P) are used to record the information compiled in determining the Ageostrophic Intensity. The ageostrophic wind speed was computed for all thermosonde launches using the following equation:

$$V - V_g = -\frac{K}{f} V^2 \quad (1)$$

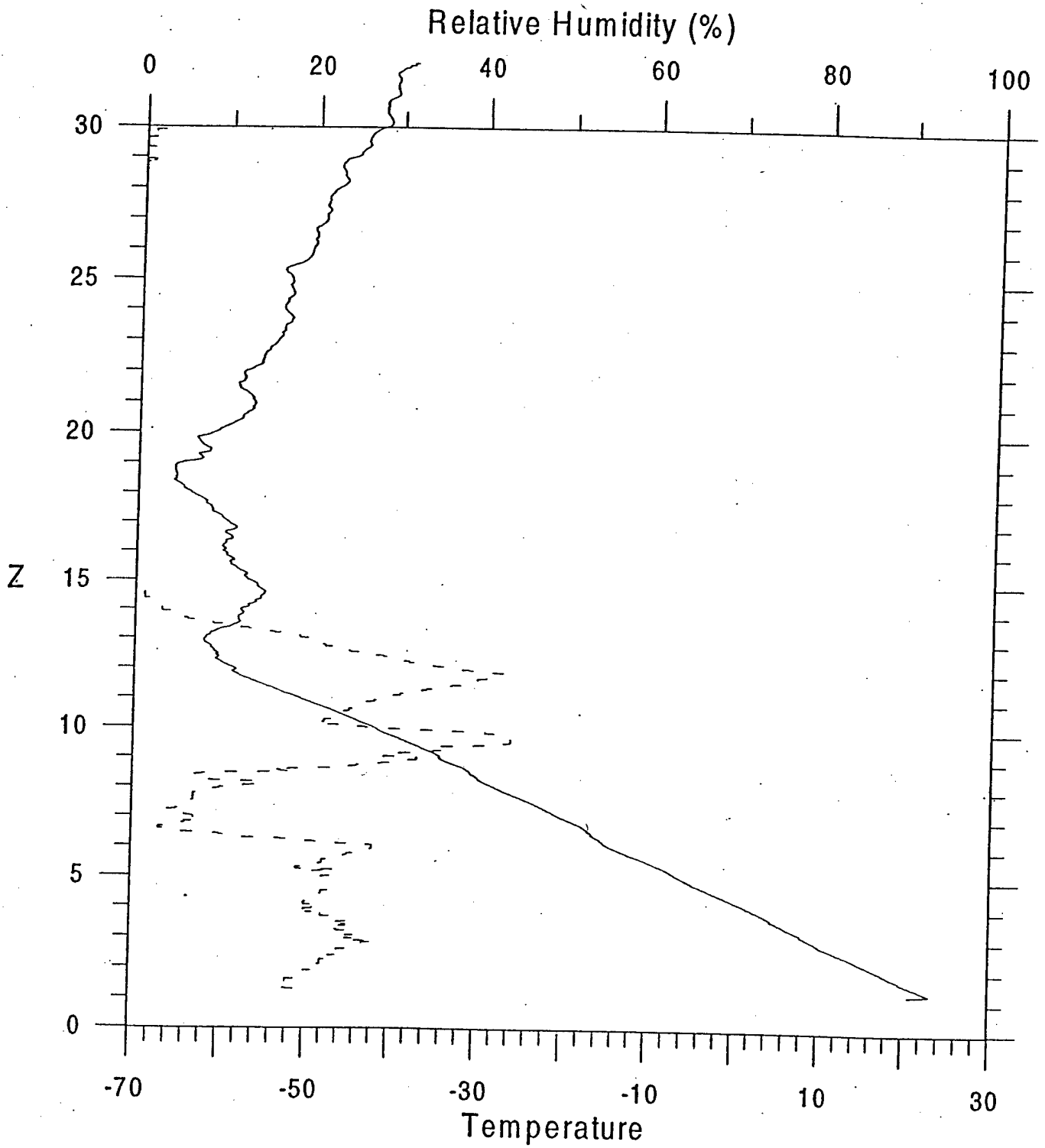


Figure 1. Temperature (C) vs. Z (Height (Km)) Solid Line and Relative Humidity (%) vs. Z (Height (Km)) Dashed Line for HMNSP107.

if $K > 0$, $V_g > V$ and where: $f = 2\Omega \sin \Phi$; $\Omega = 7.292e^{-05} s^{-1}$ and $\Phi = \textit{latitude}$.

Where V is the observed wind speed, V_g is the geostrophic wind speed, K is the inverse of the radius of curvature of the flow, and f is the Coriolis parameter ($2\Omega \sin \Phi$). K is positive if the flow is cyclonic, negative if anticyclonic. Equation (1) was evaluated for the 200 mb pressure surface using the appropriate latitude of each thermosonde launch when evaluating the Coriolis parameter. V is taken directly from the NCEP 200 mb wind speed analysis. The radius of curvature is determined graphically from the NCEP 200 mb contour analysis. This equation was evaluated and discussed in Newton and Palmen (1963)¹ and Palmen and Newton (1969)². It seems suitable for our initial approach in that it avoids errors associated with assuming that the large-scale analysis database represents an accurate measure of the “observed” wind velocity and height contour field at our scales of interest. The curvature factor K as we use it is applied to the streamline or instantaneous flow field. Strictly speaking, K applies to the flow trajectory. The difference between these two applications at 200 mb is probably small given the relatively slow movement of the synoptic-scale waves relative to the observed wind speeds.

The ratio of $(V - V_{ag})/V$ was then calculated for each profile to estimate the degree of ageostrophic forcing. This approach is patterned after the diagnosis of Koch and O’Handley (1997)³ and is designed to be a crude estimator of the degree of unbalanced flow associated with jet stream flow. Qualitative ageostrophic forcing categories were assigned to this ratio as follows: the range 0-0.2 is assigned as weak, 0.2-0.4 is moderate,

and greater than 0.4 represents strong ageostrophic forcing. Calculations of this ratio show the highest values associated with the strong subtropical jet stream or jet streak patterns. The magnitudes and sign of the computed ageostrophic wind speed also are consistent with those found in Newton and Palmen (1963).

Figure 2. is the 200 mb geopotential height chart, from the NCEP data base, used to determine the radius of curvature for ROKSU022. The radius (R) is 4.5 degrees or, approximately, 495,000 meters and is positive due to the cyclonic curvature. From the NCEP data base, the 200 mb Speed (V) for ROKSU022 is 10 m/s and the coriolis parameter (f) for Osan AB, Korea is 0.000088 s^{-1} . Substituting these values in equation (1) after solving for V_g yields:

$$V_g = \frac{V^2}{f} K + V \quad (2)$$

Substituting yields:

$$V_g = \frac{(10 \text{ m/s})^2}{(0.000088 \text{ s}^{-1})} \left(\frac{1}{495000 \text{ m}} \right) + 10 \text{ (m/s)}$$

$$V_g = 12.30 \text{ m/s}$$

The ageostrophic speed is found by subtracting the geostrophic speed from the 200 mb. speed or:

$$V_{ag} = V_g - V \quad (3)$$

Substituting yields:

$$V_{ag} = 12.30 \text{ m/s} - 10.00 \text{ m/s}$$

$$V_{ag} = 2.30 \text{ m/s}$$

The intensity of the ageostrophic forcing is determined by:

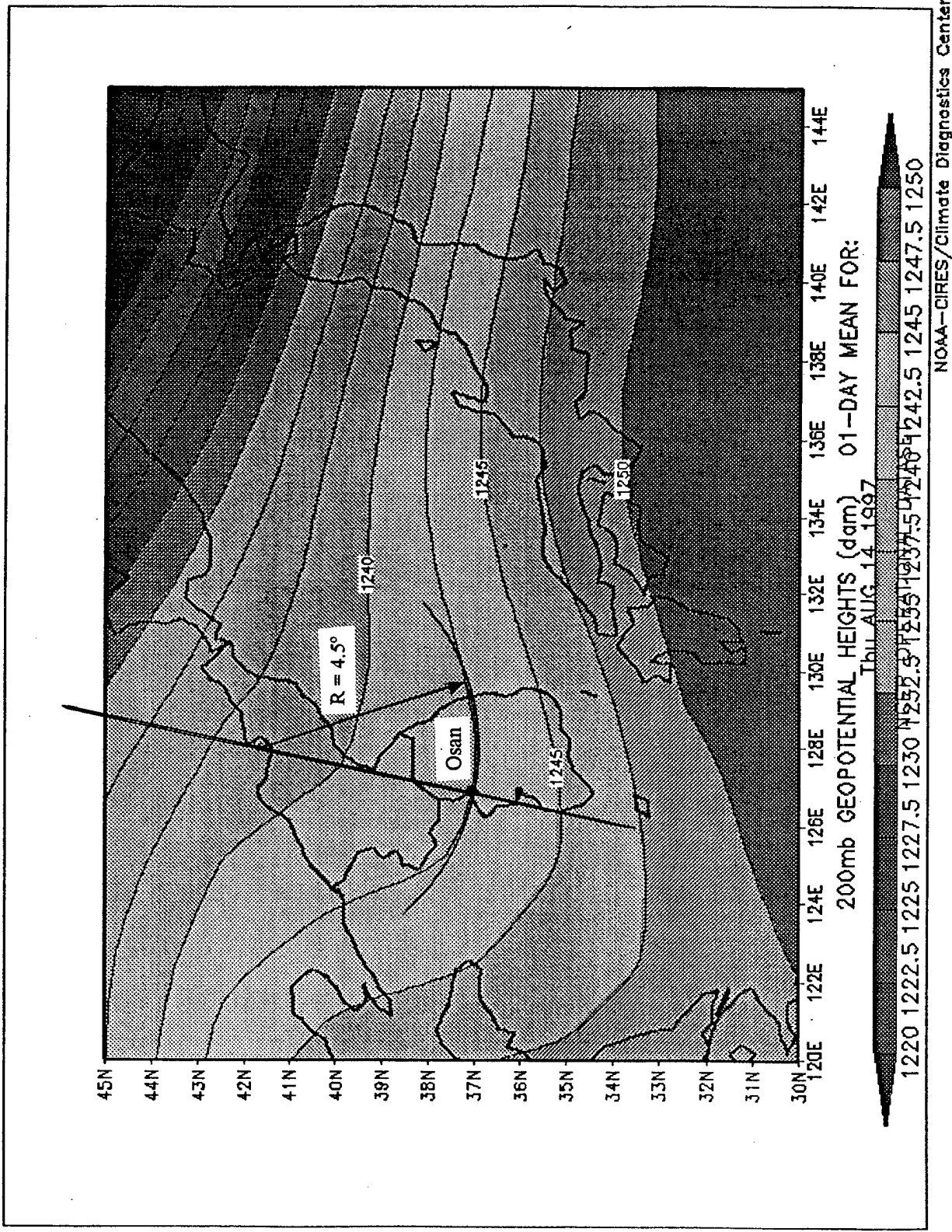


Figure 2. The 200 mb Geopotential height chart used to determine the radius of curvature for ROKSU022.

$$Intensity = \frac{|V_{ag}|}{V} \quad (4)$$

Substituting yields:

$$Intensity = \frac{2.30}{10}$$

$$Intensity = .23$$

Figure 3 is the 200 mb geopotential height chart used to determine the radius of curvature for ROKSU027. In this case the radius of curvature (R) is -4.5 degrees, negative due to the anticyclonic flow. From the NCEP data base, the 200 mb V is 7 m/s for ROKSU027 and substituting these values into equation (2) yields a value of:

$$V_g = \frac{V^2}{f} K + V$$

where: $V - V_g = -$ (cyclonic); and $V - V_g = +$ (anticyclonic)

$$V_g = \frac{(7m/s)^2}{(.00008s^{-1})} \left(\frac{-1}{495000} \right) + 7m/s$$

$$V_g = -1.12 + 7 = 5.88$$

Subsequently, substitution into equation (3) and (4) yields:

$$V_{ag} = V_g - V$$

$$V_{ag} = 5.88 - 7.00$$

$$V_{ag} = -1.12$$

and;

$$Intensity = \frac{|V_{ag}|}{V}$$

$$Intensity = \frac{|-1.12|}{7}$$

$$Intensity = 0.16$$

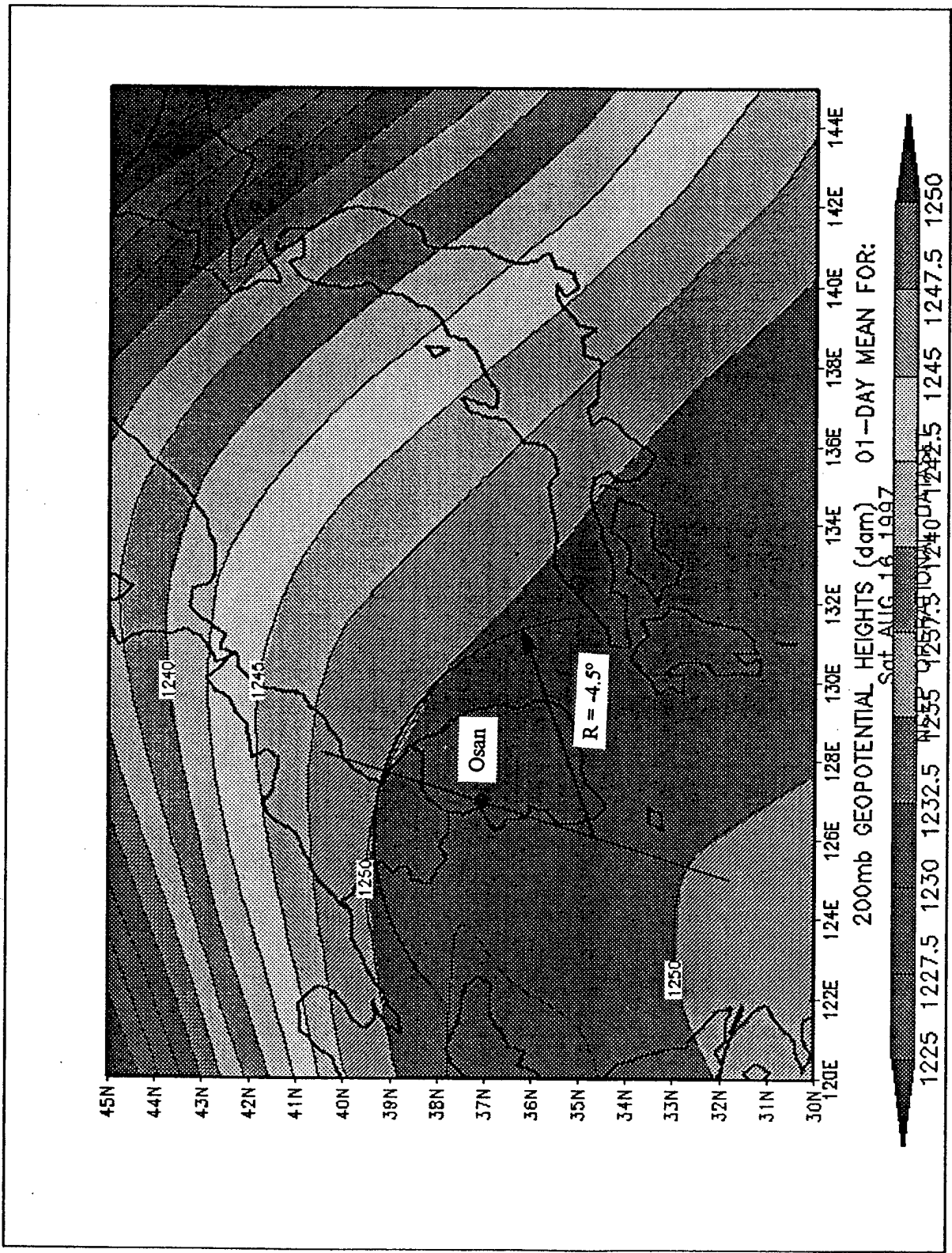


Figure 3. The 200 mb Geopotential height chart used to determine the radius of curvature for ROKSU027.

2.6. Shear Peaks

“Q”
Shear Peaks
10

Column Q lists the number of vertical shear peaks for each flight. The shear peaks were obtained by means of a “wind shear calculator” program. The program uses the “ascent_name.win” files from each balloon ascent. These text files contain three columns of data: Altitude (km), Wind Speed (m/s), and Wind Direction (degrees). The “wind shear calculator” computes and constructs graphs of the wind shear with various amounts of smoothing. A smoothing of the wind shear data points is necessary due to the large standard deviation between individual data points. Figure 4 is a plot of vertical wind shear results from four ranges of smoothing for ROKFA115 (Osan AB, Korea, 14 Mar 1997). It was decided to employ an 11-point smoothing technique for the average wind shear data listed here. Figure 5 is a plot of the 11-point smoothing of vertical wind shear data for ROKFA115. It was further decided to take values of average wind shear greater than .015 as being significant. Column Q lists the number of data points of vertical wind shear greater than .015 using an 11-point smoothing technique.

2.7. Jet Speed (m/s), Jet Altitude (km)

“R”	“S”
Jet V (m/s)	Jet Alt (km)
38.3	14.1

The Jet Speed and Jet Altitude were recorded from the wind data taken during each flight and are recorded in columns R and S. The value of Jet V differs from the value of max (m/s) in column K because the wind speed in column K is a “smoothed” value of

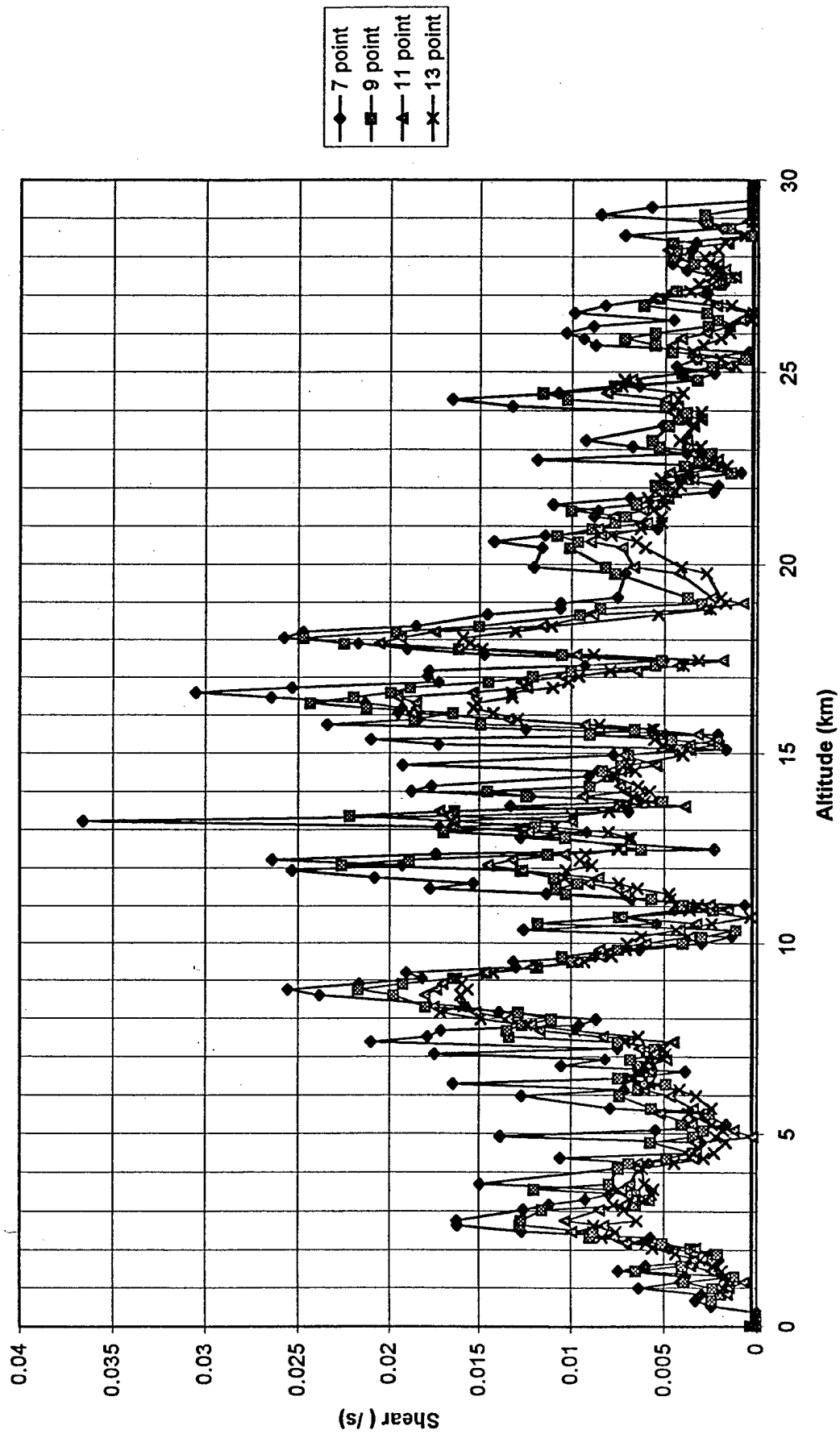


Figure 4. Vertical Shear (/s) vs Altitude (km) at 7, 9, 11, and 13 Point Smoothing for ROKFA115.

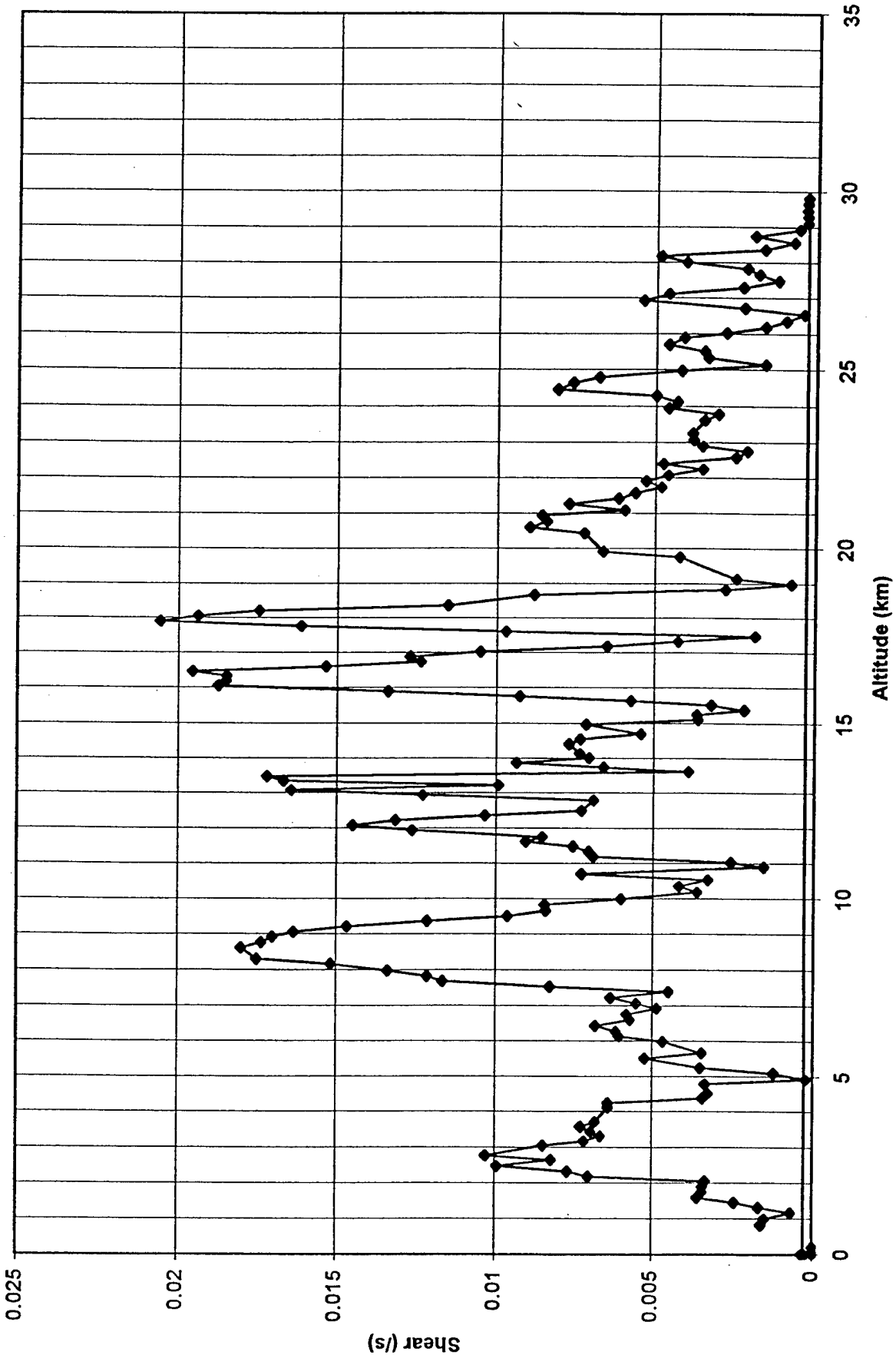


Figure 5. Vertical Shear (/s) vs Altitude (km) at 11 Point Smoothing for ROKFA115.

the wind speed data taken during the flight. Jet V and jet Alt are single data points taken from the wind profile data. Raw data points were used to get the best determination of where the balloon was located as it entered the Jet Stream area..

2.8. North, South, East, West, In Jet, Jet Type, Jet (m/s)

"T"	"U"	"V"	"W"	"X"	"Y"	"Z"
N	S	E	W	In Jet	Jet Type	Jet (m/s)
0	30	0	100	No	STJ	36

Estimates were made to determine the position of the balloon launch relative to the Jet Stream. A determination of where the balloon was, in respect to where it was launched, as it reached the Jet Stream altitude (column S) was made using the "wind shear calculator" program discussed earlier. Figure 6 is a plot of the distance traveled for ROKFA115 as generated by the "wind shear calculator" program and shows the trajectory of the balloon after launch. The NCEP data base was used to obtain plots of 200 mb winds for each flight (see Figure 7). The 200 mb wind plots were used to determine the location of the jet stream and the computed position of the balloon was added to the plot. The distance from the balloon to the core of the Jet Stream was measured (assuming 110 km distance for each degree lat/long) and recorded in columns T – W as the distance, in kilometers, N, S, E, W of the Jet core. Column X is used to record whether the balloon is in the Jet Stream or not. For a Polar Jet, a 200 mb wind of > 40 m/s was used to determine if the balloon was in the Jet Stream, while, for a Sub-Tropical Jet, a 200 mb wind of > 25 m/s was the determining factor. The 200 mb wind speed is recorded in column Z (jet (m/s)). The 200 mb wind speed was taken from the NCEP data base (see Figure 7). Finally, the Jet Type was determined by the

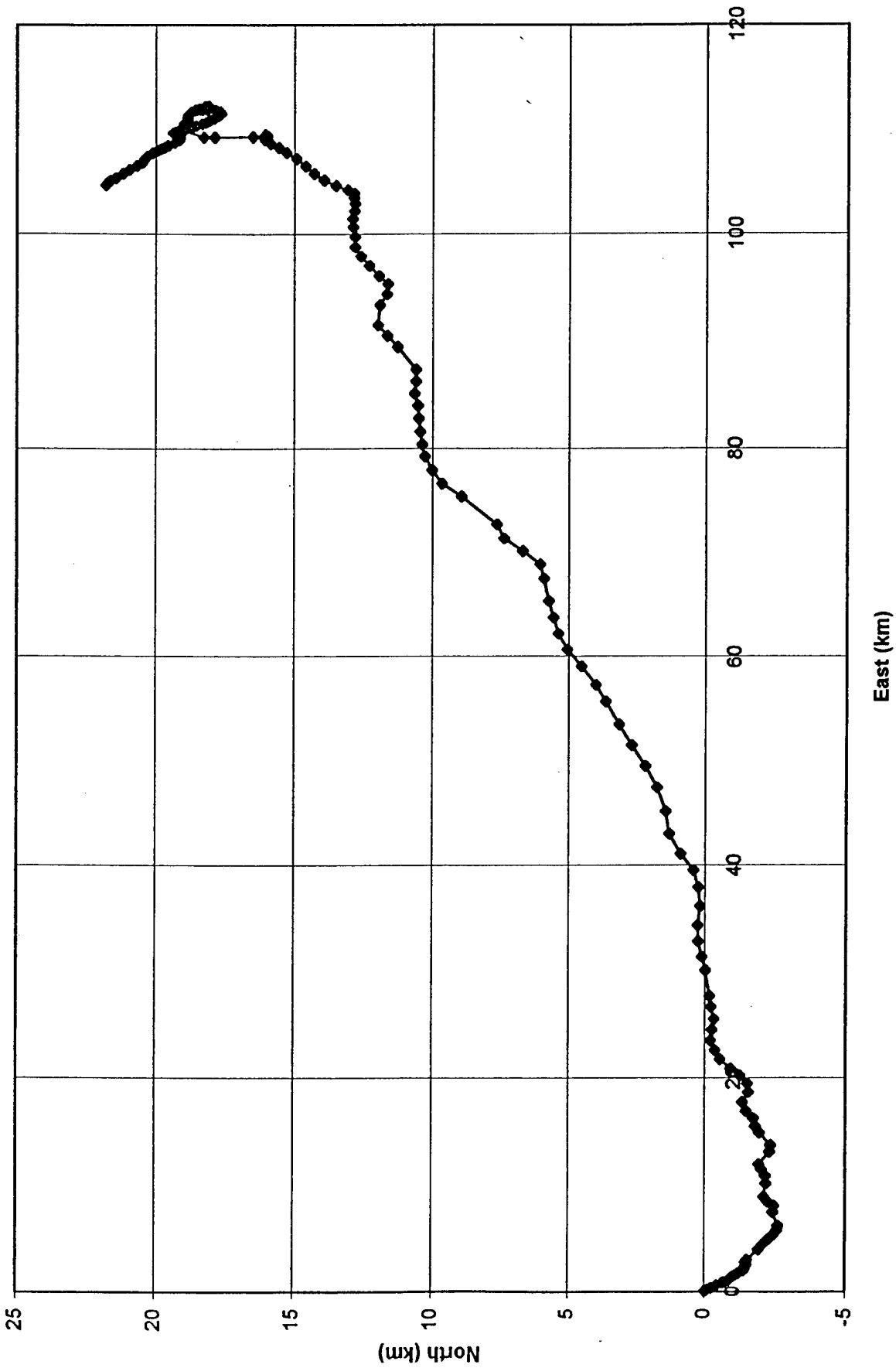


Figure 6. Path of Balloon Sounding from Surface to 38 km for ROKFA115.

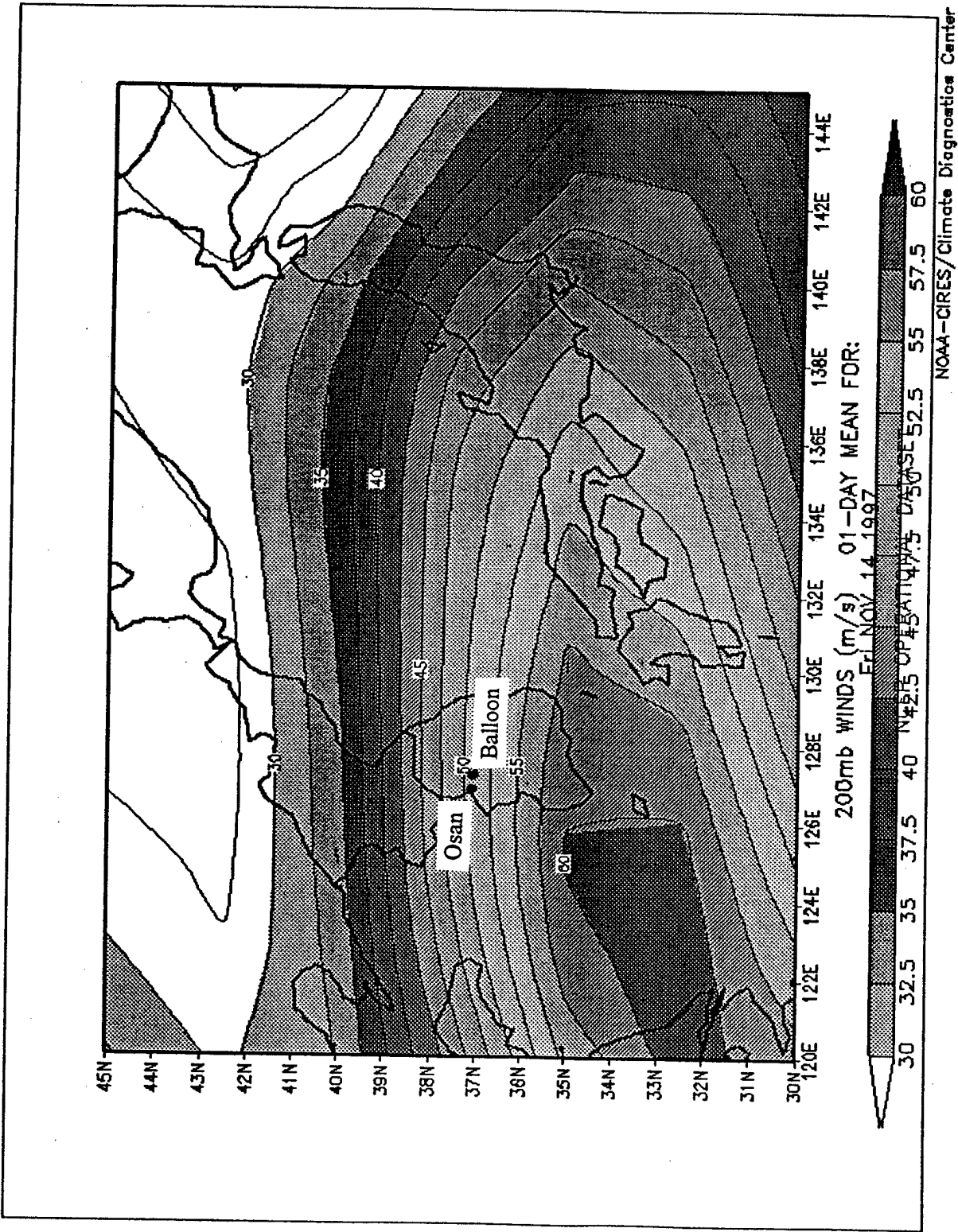


Figure 7. 200 mb Winds (m/s) for ROKFA115 Showing Site Launch and Position of Balloon at 200 mb. Level.

location of the Jet Stream, as shown on the NCEP 200 mb wind plot, and recorded in column Y. If the Jet Stream was located North of 40 degrees latitude, it was classified as a Polar Jet and if it was located South of 40 degrees latitude (Northern Hemisphere), it was classified as a Sub-Tropical Jet. There were cases when the two Jets combined and this was also recorded.

2.9. Weather, Surface Temperature (C), Frontal Passage, Sea-Level Pressure (mb), Wind (m/s), Relative Humidity (%)

“AA”	“AB”	“AC”	“AD”	“AE”	“AF”
Weather	Sfc T (C)	FROPAS	SLP (mb)	wind (m/s)	RH (%)
Partly Cloudy	39	No	1004	2	15

Columns AA to AF contain the synoptic weather conditions for each flight as close to the time of launch as possible. The data was obtained mostly from the NCEP data base. Surface temperature, sea-level pressure, surface wind speed and relative humidity were taken directly from the NCEP data base while the weather and frontal passage data were either inferred from the NCEP data base or acquired from the synoptic notes taken for about half of the flights by a meteorologist at the site. These notes are also recorded in the comments contained in the last column (AO).

2.10. Jet Enhancement, Tropospheric Enhancement, Stratospheric Enhancement

“AG”	“AH”	“AI”
Jet enhance	trop enhance	strat enhance
no	strong	no

A determination was made as to whether there was enhancement of C_n^2 caused by the Jet Stream, the Tropopause or the Stratosphere. If there was enhancement, it was recorded as strong or weak in columns AG, AH, and AI. The enhancement was determined by comparing the plot of C_n^2 vs Z to the CLEAR 1 model. Figure 8 is the plot of C_n^2 vs Z for flight HMNSP104 (14 May 1998) taken at Holloman AB, New

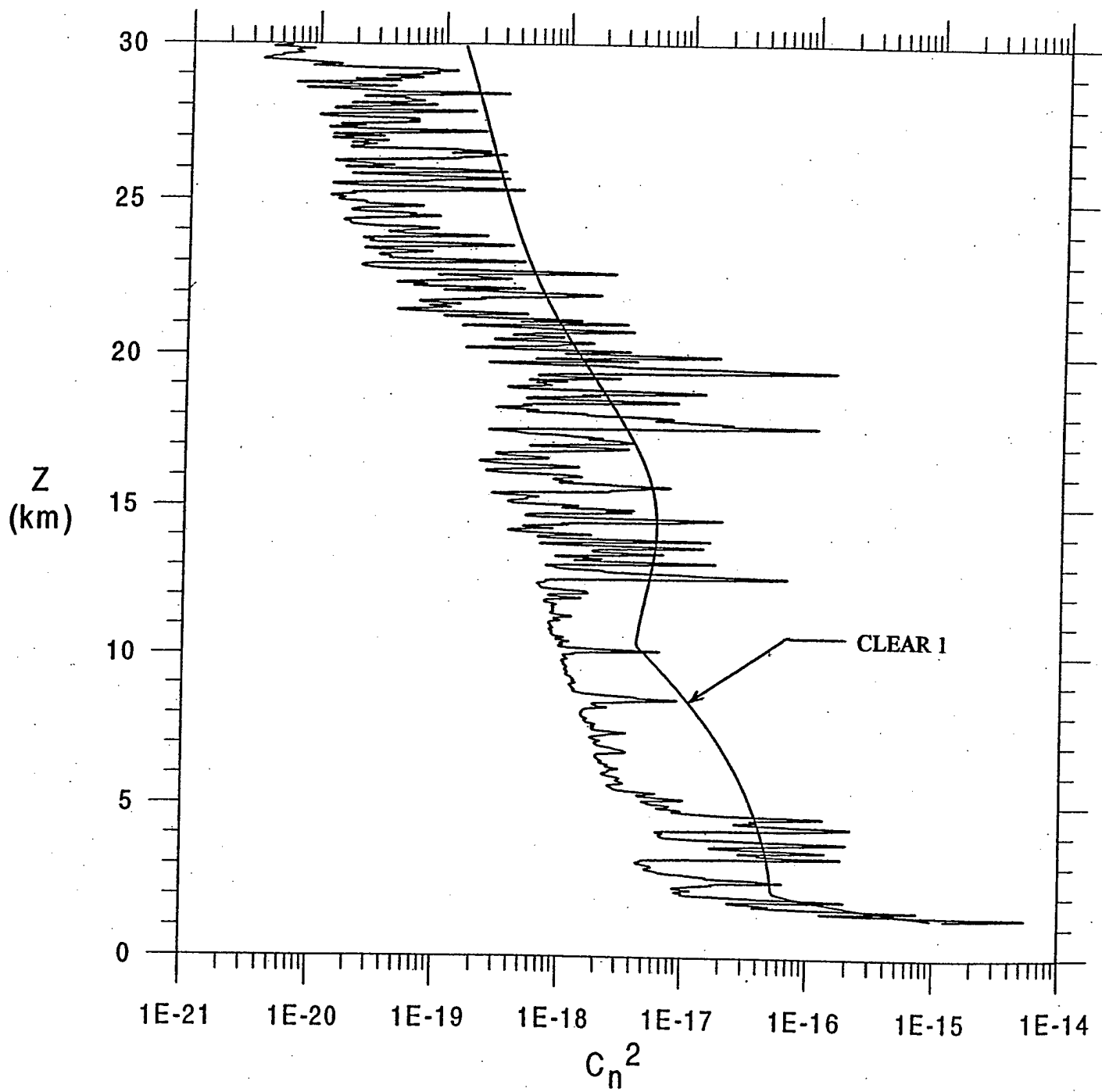


Figure 8. C_n^2 (20m Gaussian Average) vs Z (Height (km)) for HMNSP104.
 CLEAR 1 Model Superimposed for Comparison.

Mexico. For this flight, there is no evidence of jet enhancement (taken from column X which has a negative since 200 mb wind speed was $< 25\text{m/s}$), but the values of C_n^2 are significantly larger at the tropopause region (13 and 19 km. from columns H and I) than the CLEAR 1 model. Above the tropopause (20 km.), values for C_n^2 are lower than CLEAR 1, therefore, there is no stratospheric enhancement.

2.11. Deformation, Intensity

“AJ”	“AK”
deformation	intensity
4.37	Light

A deformation term was calculated for each flight and is shown in column AJ. The deformation term was used to obtain a measure of the horizontal shear. From Saucier (1955)⁴ the following equation was used:

$$|DEF| = \left[\left(\frac{\partial u}{\partial x} - \frac{\partial v}{\partial y} \right)^2 + \left(\frac{\partial v}{\partial x} + \frac{\partial u}{\partial y} \right)^2 \right]^{\frac{1}{2}} \quad (5)$$

Appropriate values of u and v were obtained from the NCEP data base. Figure 9 is the plot of u for ROKSP101 (Osan AB, Korea, 5 May 1998). A circle of radius 2 degrees was drawn at the position of the launch and values of the change of u in the x (W-E) and y (S-N) direction was measured from the plot. For flight ROKSP101, du/dx is 40 – 28 or 12 m/s and du/dy is 28 – 40 or –12 m/s. In a similar manner values of v were obtained (see Figure 10). For ROKSP101, dv/dx is 12.5 – 1 or 11.5 m/s and dv/dy is –1.25 – 14.5 or –15.75. Substituting these values into equation (5) yields:

$$|DEF| = \left[(12 - (-15.75))^2 + (11.5 + (-12))^2 \right]^{\frac{1}{2}}$$

$$|DEF| = \left[(27.75)^2 + (-.5)^2 \right]^{\frac{1}{2}} \text{ and } |DEF| = 27.75.$$

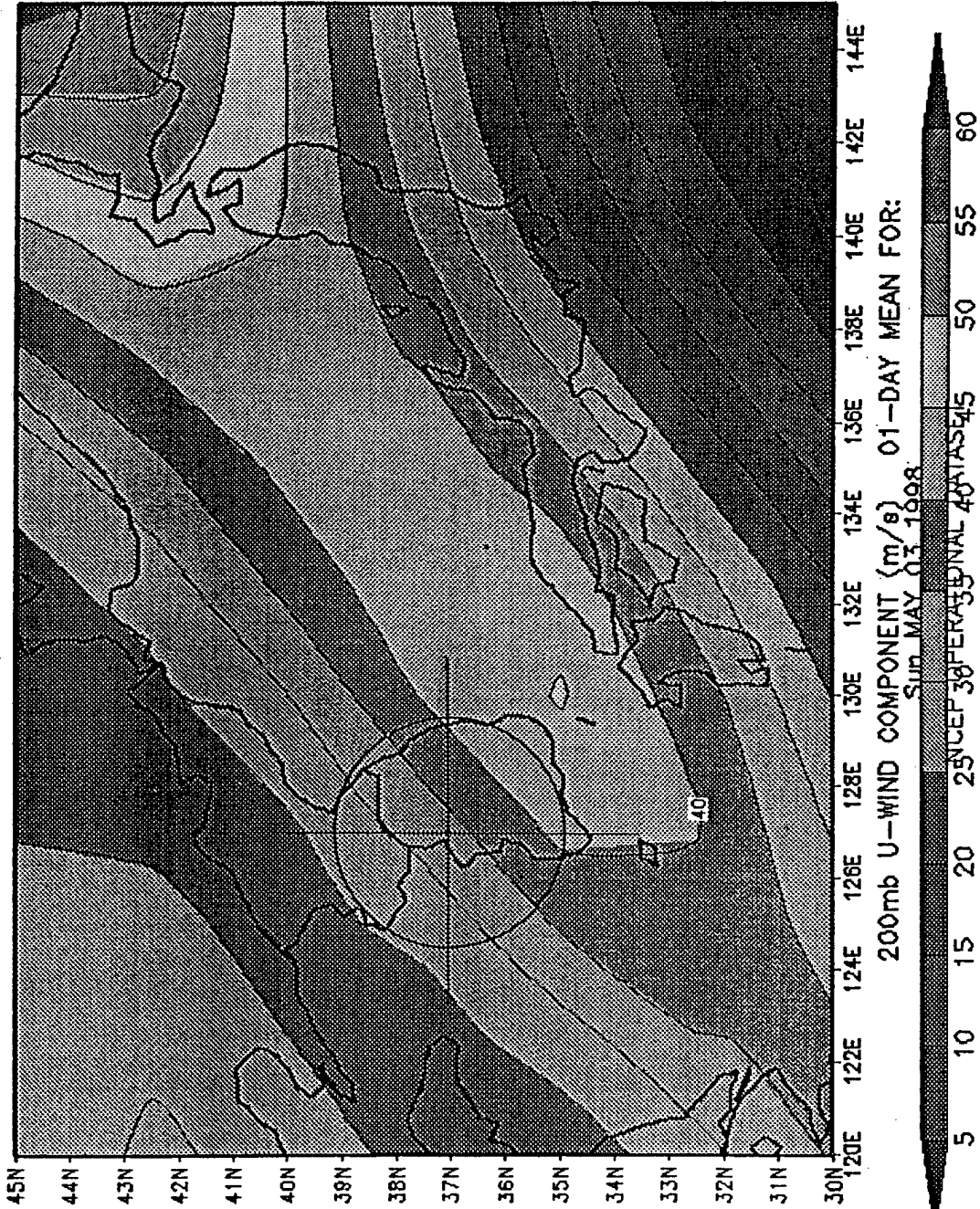


Figure 9. 200 mb U-Wind Component (m/s) for ROKSP101 with 2° Latitude Radius Circle Drawn over Osan AB, Korea.

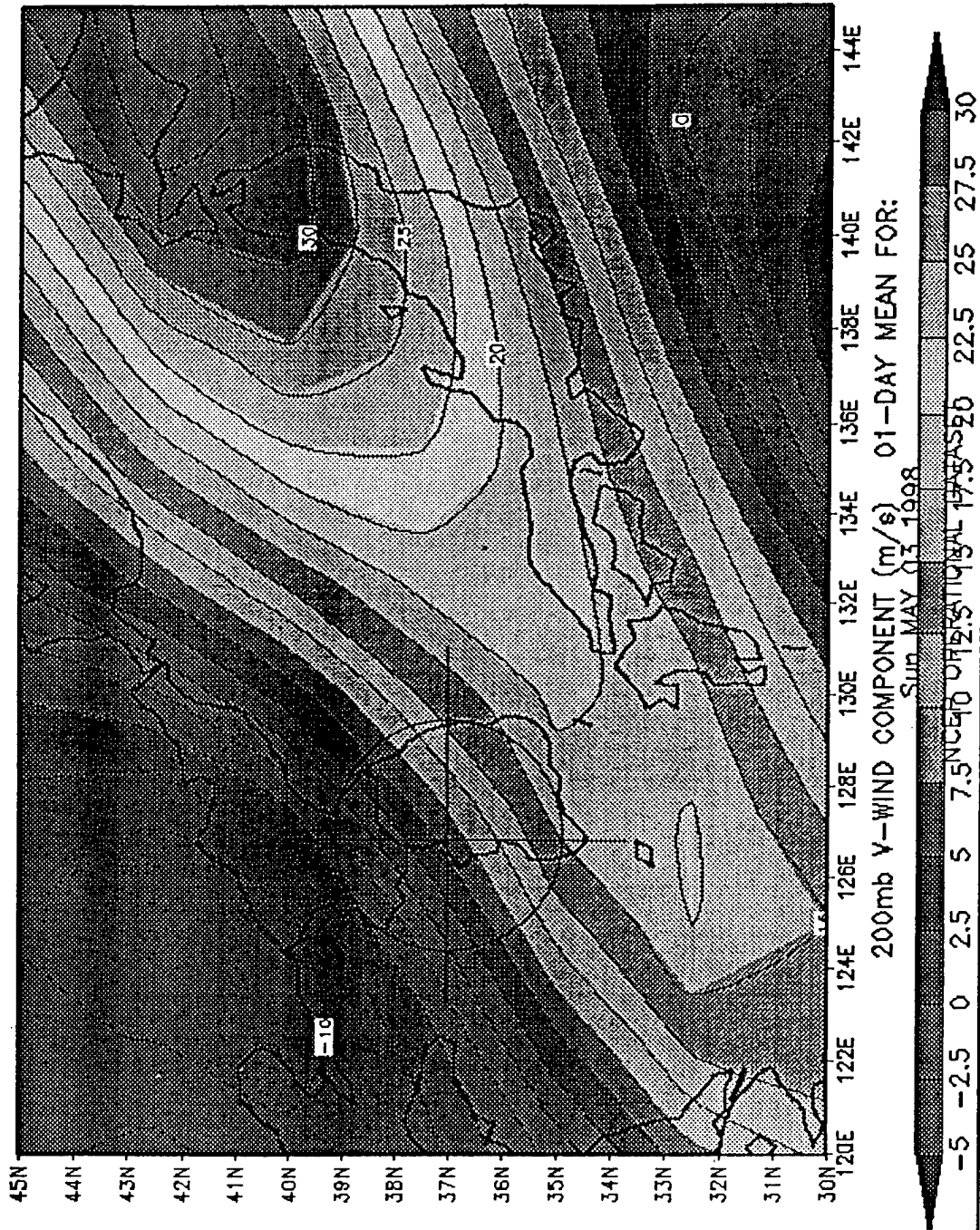


Figure 10. 200 mb V-Wind Component (m/s) for ROKSP101 with 2° Latitude Radius Circle Drawn over Osan AB, Korea.

Based on results from Mancuso and Endlich (1966)⁵ , values up to 10 were considered light deformation, between 10 and 20 were moderate and greater than 20 were considered strong deformation. The intensity of deformation is listed in column AK.

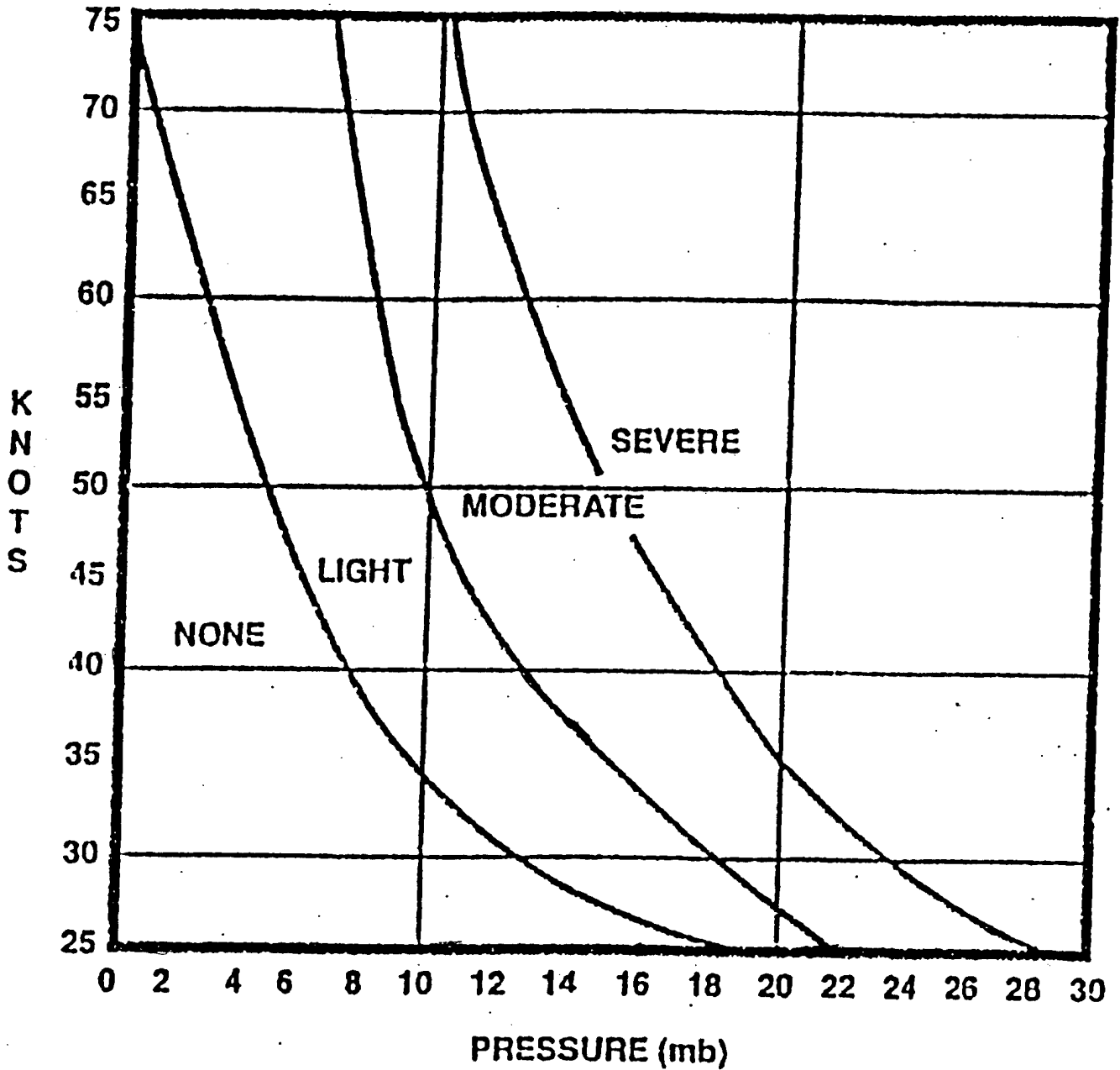
2.12. Mountain Wave Intensity

“AL”
Mtn wave inten
Light

Column AL lists the mountain wave intensity for flights where mountain ranges were present and the possibility of a mountain wave existed. For this data base, mountain waves were examined for Korea and Holloman. The approach employed was to use a nomogram from the Air Force Weather Agency manual AFWA TN-98/0002, 15 Jul 1998, Meteorological Techniques (see Figure 11).

The mountain wave nomogram method predicts mountain wave intensity qualitatively in categories: none, light, moderate, and severe as a function of maximum wind speed below 500 millibars and sea level pressure differential across the mountains. For our analysis, the pressure differential is calculated simply by subtracting the east Korean coast sea level pressure from the west Korean coast sea level pressure determined from weather maps. The 500 mb and below wind data are taken from thermosonde measurements. For Holloman, the boundary (E-W) of the state of New Mexico was used to determine pressure differential. The wind direction was also taken into account since a wind perpendicular to the mountain range would give a full effect, while a wind parallel to the mountain range would have no effect. For Korea and Holloman a westerly wind (270 degrees) was considered to be perpendicular to the mountain range.

MOUNTAIN-WAVE NOMOGRAM



KNOTS = Maximum Wind Speed Below 500mb
PRESSURE = Sea-level Pressure Differential Across Mountains

Figure 11. Mountain - Wave Nomogram Used to Determine Mountain - Wave Intensity.

2.13. Aircraft, RFI, Comments

"AM" aircraft n	"AN" RFI n	"AO" comments (as stated)
-----------------------	------------------	----------------------------------

If an aircraft was employed to supplement the flight it is entered in column AM. In some launches, radio frequency interference (RFI) was a problem and if this was the case it was noted in column AN. The last column (AO) contains comments made by the launch team at the time of the launch. These comments have been preserved from their initial entry.

3. OPTICAL TURBULENCE DATA REDUCTION AND STORAGE

Validated data from individual balloon ascents has been averaged into altitude bins and stored in the table "Altitude Bins" in the Master Database.

3.1 Data Source

The source of the turbulence data for the Database is the standard "dot-text" files for the individual ascent profiles. This file is not the raw data from the radiosonde, but one of the many files created in the data reduction process. This particular file is in a form that is usually required for atmospheric characterization for optical propagation calculations. The files are validated in the sense that they are carefully checked and known file defects such as excessive noise and baseline drift are eliminated. An excerpt from a text file follows:

0.0116	1022.8998	3.8000	68.0000	4.8134e-015
0.0227	1021.5002	3.8000	68.0000	1.2535e-014
0.0323	1020.2997	4.1000	68.0000	1.6684e-014
0.0379	1019.5999	4.3000	68.0000	1.0248e-014
0.0451	1018.7002	4.6000	67.0000	5.6553e-015
0.0515	1017.9002	4.8000	67.0000	3.7696e-015

The columns are: altitude (km) above sea level , pressure (mb), temperature ($^{\circ}\text{C}$), relative humidity (%), and the structure constant for index of refraction, C_n^2 ($\text{m}^{-2/3}$). The lines represent data for each line of telemetry, which is received at intervals of 1 to 2 seconds, depending on the radiosonde used for the experiment. These files can vary in length from 3000 to 6000 lines, and contain much more precision than is usually required for optical calculations. For any ascent, there may be missing values at the beginning, at the end, or anywhere in-between. This could be due to telemetry dropouts or other problems.

3.2 Data Preparation for Table

One of the first decisions that had to be made to assemble the database was the best thickness in altitude to be used for storage. By averaging the C_n^2 for larger and larger altitude bins, it was determined that the precision of a Rytov variance calculation did not begin to seriously degrade until the bins became thicker than 500m. After further consideration, it was decided to use a 150m bin size, which is the same size that is used for WSMR radar data. Further, the bins were all aligned such that identical altitude ranges would be used for each bin, so that such calculations such as the mean turbulence for a given altitude could be easily computed. Finally, the altitudes used were chosen to be identical to those used for the WSMR radar data. The bottom altitude for the first bin is 3.222 km, the top of the first bin is 3.372 km, and the nominal altitude in the file is the mean, 3.297 km. The last bin was at a nominal altitude of 29.997 km, since balloon data were typically disregarded above 30 km. The balloons usually burst around that altitude, and there is a question about the accuracy of the measurements above that altitude due to heat transfer considerations.

The Thermosonde actually measures the structure constant for temperature, C_T^2 . This

quantity is then converted to C_n^2 using the formula:

$$C_n^2 = \left(79 \times 10^{-6} \frac{P}{T^2} \right)^2 C_T^2 \quad (6)$$

where P is pressure in mb, T is temperature in K, and C_T^2 is in $K^2 m^{-2/3}$

The atmospheric conditions in the multiplier impose decreasing C_n^2 values with altitude, while minimum and maximum C_T^2 excursions remain relatively constant with altitude. Therefore it was decided to convert C_n^2 back to C_T^2 prior to averaging over altitude. The average for bin j is the mean value of an assumed continuous function defined by the formula:

$$\bar{C}_{Tj}^2 = \frac{\int_{z_{j1}}^{z_{jn}} C_T^2(z_j) dz}{z_{jn} - z_{j1}} \quad (7)$$

where z is the altitude, z_{j1} is the minimum altitude within the bin j, and z_{jn} is the maximum altitude in the bin j. The numerical integration is performed using the trapezoid rule. Since the lower and upper altitudes of the bin do not usually occur at the data altitudes, the values for the z_{j1} and z_{jn} are estimated by linear extrapolation of the bounding lines of data. There must be at least three lines of data within the bin for the bin to be considered in the database. If a bin is not valid for lack of the required data, the bin is not entered into the database.

Means are also calculated for temperature and pressure, with the purpose of recomputing a valid value of C_n^2 . With this in mind, it is the mean value based on P^2 and the mean value based on T^4 that is computed. Each line in the Altitude Bins table, contains the balloon flight identifier, and mean values of altitude, C_T^2 , P, T, and C_n^2 .

Note that the temperature mean (T^4) is computed using degrees Kelvin, then it is

converted back to Celsius. There is also a unique key number automatically assigned to each entry line by the program. A sample of the table is shown below.

Table 2. Table of Flight Bins and Computed Means.

	FLIGHT	BIN ALT	CT2 MEAN	p MEAN	T MEAN	Cn2 MEAN
64433	roksu020	12.897	0.0000163820	187.1999	-50.2838	1.4523E-18
64434	roksu020	13.047	0.0000141660	182.9569	-51.4488	1.2249E-18
64435	roksu020	13.197	0.0000098820	178.7895	-52.4193	8.3048E-19
64436	roksu020	13.347	0.0000110490	174.6991	-53.6162	9.0608E-19
64437	roksu020	13.497	0.0000089451	170.6789	-54.7668	7.1503E-19
64438	roksu020	13.647	0.0000073323	166.7330	-55.8024	5.7006E-19

In a typical use of the database, a selection is made for either a single flight, or a group of flights based on conditions in the Master Flights Table. Next the desired data are extracted from the Altitude Bins Table using a query. Finally calculations are made using the extracted data. A simple example calculation is the mean C_n^2 for each altitude bin, which can be accomplished using the AVG function built into the database.

4. CAMPAIGN SUMMARY TABLE

The campaign summary table consists of the following: campaign designator for the flight identification number, campaign location, date of first and last balloon launch of the campaign, and number of flights entered into the database. There are also check boxes to indicate completion of data entry into the Master Flight Table, the Altitude Bins Table, if the campaign had contemporaneous airborne data collections, and if the data had been through the quality control procedure. A convenient way to view these data is to call up the Campaign Summary Form, which displays the data from each campaign on a single window.

5. CONCLUSION

In compiling the Master Data Base, every attempt was made to use thermosonde measured values wherever possible. In doing this, it is hoped that the accuracy of the Master Data Base could be kept at the highest possible level. However, some of the parameters, i.e., deformation, ageostrophic wind, mountain wave, etc., had to be computed for large scale analyses. Where this was necessary, methodologies were employed that retained the highest possible accuracy and the results were considered as accurately as possible. For example, actual deformation values were determined but were then recorded as qualitative values as light, moderate and strong intensities. Furthermore, all the parameters that could be garnered from the actual flight data were used and recorded in raw form. This allows future analysis to be performed should new ideas evolve in the overall ABL study. The Master Data Base is considered a good summary of the numerous weather related parameters occurring during the entire ABL field program to date and can easily be updated to include additional research data. The Altitude Bins Table contains optical turbulence parameters C_n^2 and C_T^2 along with the mean altitude, mean pressure and mean temperature of each flight bin with at least 3 interior data records. The Campaign Summary Table is a good first table to use to determine what campaigns are part of the database, and the status of the data reduction. The C_n^2 Master database also contains many forms that are reports which should be useful in viewing and reporting information.

References

1. AFWA TN-98/002, 1998: *Meteorological Techniques*. Air Force Weather Agency, Offutt AFB, NE, 242 pp.
2. Koch, S.E., and C. O'Handley, 1997: Operational forecasting and detection of mesoscale gravity waves. *Wea. and Forecasting*, 12, 253-281.
3. Mancuso, R.L., and R.M. Endlich, 1966: Clear air turbulence frequency as a function of wind shear and deformation. *Mon. Wea. Rev.*, 94, 581-585.
4. Newton, C.W., and E. Palmen, 1963: Kinematic and thermodynamic properties of a large-amplitude wave in the westerlies. *Tellus*, 15, 99-119
5. Palmen, E., and C.W. Newton, 1969: *Atmospheric Circulation Systems: Their Structure and Physical Interpretation*. Academic Press, New York, 603 pp.
6. Saucier, W.J., 1955: *Principles of Meteorological Analysis*. Univ. of Chicago Press, Chicago, 438 pp.
Reap, R.M., 1989: 24-H NGM Based Probability and Categorical Forecasts of Thunderstorms and Severe Local Storms for the Contiguous U.S., *NWS Technical Procedures Bulletin*, Series No. 419. 2.